Jorge Rencoret*, Ana Gutiérrez, Eulogio Castro and José C. del Río

Structural characteristics of lignin in pruning residues of olive tree (*Olea europaea* L.)

https://doi.org/10.1515/hf-2018-0077
Received April 6, 2018; accepted September 13, 2018; previously published online October 13, 2018

Abstract: Olive tree pruning (OTP) is an abundant and inexpensive agricultural lignocellulosic residue that is an interesting feedstock for producing bioethanol and other bio-products in the context of lignocellulosic biorefineries. However, the presence of lignin in OTP hinders the transformation processes as it limits the access to cell wall polysaccharides. On the other hand, the aromatic/phenolic structure of the lignin polymer makes it an interesting raw material for producing chemicals, fuels and other commodities that are nowadays produced from fossil fuels. Thus, the knowledge of the OTP lignin structure is crucial to develop tailor-made pretreatments for their removal as well as for additional valorization of the lignin polymer. In this work, the OTP lignin was isolated as milled wood lignin (MWL), a lignin preparation that is considered representative of the native lignin, and characterized by two-dimensional nuclear magnetic resonance (2D-NMR) and thioacidolysis. The results demonstrated that the lignin is mainly composed of guaiacyl (G) and syringyl (S) lignin units in similar abundances (S/G ratio of ~1), with minor amounts of *p*-hydroxyphenyl (H) units. The most abundant lignin inter-unit linkages are β-*O*-4′ alkyl-aryl ethers (75% of all linkages), followed by the condensed phenylcoumarans (12%) and resinols (8%), and with lower amounts of dibenzodioxocins (2%) and spirodienones (3%). The analysis of the thioacidolysis dimers gave additional information regarding the distribution of the lignin units involved in condensed interunit linkages, including 5-5′, 4-*O*-5′, β-5′, β-1′ and β-β′. The high lignin content (25%), together with the relatively low S/G ratio and the abundance of condensed (carbon-carbon linked) structures, points to a low reactivity of OTP lignin during delignification pretreatments.

Keywords: 2D-NMR, lignin, milled wood lignin (MWL), olive tree pruning, thioacidolysis

***Corresponding author: Jorge Rencoret,** Instituto de Recursos Naturales y Agrobiología de Sevilla, CSIC, 41012-Seville, Spain, Tel.: +34 954624711, e-mail: jrencoret@irnase.csic.es.
https://orcid.org/0000-0003-2728-7331
Ana Gutiérrez and José C. del Río: Instituto de Recursos Naturales y Agrobiología de Sevilla, CSIC, 41012-Seville, Spain.
https://orcid.org/0000-0002-8823-9029 (A. Gutiérrez);
https://orcid.org/0000-0002-3040-6787 (J.C. del Río)
Eulogio Castro: Department of Chemical, Environmental and Materials Engineering, University of Jaén, 23071-Jaén, Spain.
https://orcid.org/0000-0003-1719-6049

Introduction

Olive tree (*Olea europaea* L.) is the most popular member of the Oleaceae family and it is among the most extensively cultivated fruit crops in the world, covering more than 10.6 M ha, 95% of which are located in the Mediterranean region (FAOSTAT, 2016). Every 2 years after olive harvesting, pruning of mature olive trees is required to renew the fruiting surface and achieve high yields, maintain vegetative growth of fruiting shoots, favor light penetration and air circulation inside the canopy, prevent aging of the canopy and to eliminate dead wood. Taking into account the estimation that around 3 t ha^{-1} of olive tree residues (including leaves, thin branches and wood) are produced per year (Sánchez et al. 2002), olive tree prunings (OTPs) annually generate up to 34.5 M t of pruning residues. The OTPs are a largely unexploited agricultural residue that accumulates in the field, and which are usually mulched or burned (Romero et al. 2010). However, OTP could be an interesting raw material for lignocellulosic biorefineries due to its low cost and widespread availability and high carbohydrate content (Cara et al. 2008; Romero et al. 2010; Díaz et al. 2011; Toledano et al. 2011; Santos et al. 2017). Biorefinery is a concept for biomass utilization by separating and transforming cellulose, hemicelluloses, and lignins into value-added bioproducts and biofuels in high yields in an economic and sustainable manner (Ragauskas et al. 2006; Himmel 2008).

Lignins are barriers to the efficient utilization of plant polysaccharides beginning with ruminant digestibility and ending up with industrial processes such as pulping and other biorefinery processes. On the other hand, lignin itself is a valuable polyaromatic compound. The most challenging step in biorefinery processes is the removal of lignin and to break down its polymeric structure responsible for the poor accessibility of polysaccharides to chemicals or enzymes. To this end, pretreatment methods were developed taking into consideration the specific details of a tree or plant. Lignin as a branched

and partly cross-linked aromatic copolymer consists mainly of three different phenylpropane units, namely *p*-hydroxyphenyl (H), guaiacyl (G) and syringyl (S) units, which are linked by ether and carbon-carbon bonds (Boerjan et al. 2003; Ralph et al. 2004). The content and composition of lignins vary widely depending on the type of lignocellulosic material, age, cell types and environmental conditions (Zobel and van Buijtenen 1989). To learn more about the way how lignins are inhibiting the polysaccharides evaluation, knowledge of their structure is of primary importance.

Several studies regarding the chemical characterization of the lignin from OTP have been published during the last years, although all of them have been devoted to the technical lignins isolated after different pretreatment methods, such as steam explosion, organosolv and alkaline pulping, and autohydrolysis (Toledano et al. 2013a,b; Santos et al. 2017; Sequeiros and Labidi 2017). Such materials, however, have a largely altered structure compared to the native lignins in the cell wall.

The aim of the present work was to characterize the native OTP ligin by *in-situ* two-dimensional-heteronuclear single quantum coherence-nuclear magnetic resonance (2D-HSQC-NMR) spectroscopy in the gel state (Kim et al. 2008; Rencoret et al. 2009a). Moreover, for a more detailed characterization, milled wood lignin (MWL) was isolated by aqueous dioxane extraction from finely ball-milled samples according to Björkman (1956). MWL is considered to be only moderately altered compared to the native lignin (Fujimoto et al. 2005; Rencoret et al. 2009a), and therefore OTP-MWL was also analyzed by 2D-NMR spectroscopy and thioacidolysis degradation. The expectation is that the collected data will contribute to tailor-made OTP pretreatments for the sake of a more effective utilization of this important agricultural feedstock.

Materials and methods

Samples: The OTPs (*Olea europaea* L., Picual variety), composed of thin branches (<5 cm diameter), were collected after fruit-harvesting from a local orchard in Jaén, Southern Spain. The samples were manually debarked, chipped, homogenized, air-dried and grounded in a IKA MF10 knife mill (IKA, Staufen, Germany) to pass 1 mm screen. The air-dried samples were then successively Soxhlet extracted with acetone (8 h), methanol (8 h) and water (3 h). Finally, the extractive free samples were finely ball-milled in a Restch PM-100 planetary mill (Retsch, Haan, Germany) equipped with a 500 ml agate jar and agate balls (20 × 20 mm), at 400 rpm, during 10 h (alternating 10 min of pause every 20 min of milling). The Klason lignin content was estimated as the residue after sulfuric acid hydrolysis of the pre-extracted material, corrected for ash and protein content, according to the TAPPI method T222 om-88 (Tappi, 2004). The acid-soluble lignin was determined at 205 nm based on the extinction coefficient of 110 l cm^{-1} g^{-1}. The average yields of three replicates are presented.

Milled wood lignin (MWL) according to Björkman (1956): Around 50 g of ball-milled material were extracted with 1 l of dioxane-water (96:4, v/v) under continuous stirring in the dark for 24 h. The solution was centrifuged and the lignin containing supernatant was collected. The extraction process was repeated twice with fresh dioxane-water solution each time and the supernatants were combined and subsequently evaporated at 40°C at reduced pressure until dryness. The crude MWL was then purified according to the solubilization/precipitation procedure described elsewhere (del Río et al. 2012). The MWL yield was around 20% of the total lignin content.

2D-NMR analyses: One hundred milligram of finely ball-milled OTP sample (the whole cell wall, OTP_{total}) were swelled in 0.75 ml of DMSO-d_6 and the resulting gel was submitted to spectroscopy according to the literature (Kim et al. 2008; Rencoret et al. 2009a). In the case of MWL, 50 mg of sample was completely dissolved in 0.75 ml of DMSO-d_6, forming a clear solution. 2D-NMR-HSQC experiments were recorded at 300K on an AVANCE III 500 MHz instrument (Bruker, Karlsruhe, Germany) fitted with a 5 mm TCI gradient cryoprobe at the NMR facilities of the General Research Services of the University of Seville. The HSQC spectra were acquired using the standard adiabatic pulse program of Bruker "hsqcetgpsisp2.2". The spectra were obtained from 10 to 0 ppm in ^{1}H dimension, with acquisition times of 145 ms (MWL) and 100 ms (OTP_{total}) and a recycle delay (d1) of 1 s. For the ^{13}C dimension, the spectral width was from 165 to 0 ppm, being collected 256 increments of 32 scans for total experiment times of 2 h 40 min and 2 h 34 min for MWL and gel sample, respectively. The $^1J_{CH}$ used was 145 Hz. Processing is based on the typical matched Gaussian apodization in ^{1}H (LB = −0.1 and GB = 0.001) and a squared cosine bell in ^{13}C (LB = 0.3 and GB = 0.1). The signal of residual DMSO served as an internal reference (δ_C/δ_H 39.5/2.49). Lignin correlation signals in the HSQC spectrum of the OTP-MWL were assigned according to the literature (Rencoret et al. 2008, 2018; Ralph et al. 2009; Lourenço et al. 2015). A semi-quantitative analysis of lignin units and linkages, based on measuring the contour volume integrals of correlation signals, was performed according to Rencoret et al. (2013). Concerning the aromatic signal evaluation of $S_{2,6}$, $H_{2,6}$, the integrals were halved to get the equivalent for the G_2 signal. The different inter-unit linkages were quantitated via the volume integrals of the A_α, B_α, C_α, D_α and F_α correlation signals, corresponding to chemically analogous C_α/H_α with similar $^1J_{CH}$ coupling values. The relative abundance of cinnamyl alcohol end-groups (I) were estimated by integration of the signal I_γ, whereas the abundance of cinnamaldehyde end-groups (J) was determined by integrating the signal J_β and comparing it with I_β.

Thioacidolysis and subsequence Raney-nickel desulphuration of MWL: The method was described by Rolando et al. (1992). The reagent was immediately prepared before use by pouring 0.25 ml of BF_3 etherate and 1 ml of ethanetiol into a 10 ml flask containing some dioxane (1–2 ml), and the final volume was adjusted to 10 ml with dioxane resulting in a 0.2 M BF_3 etherate in dioxane/ethanethiol (8.75:l, v:v) solution. 5 mg of MWL were treated with 5 ml of thioacidolysis reagent in a 10 ml screw-cap reaction vial under N_2 at 100°C during 4 h with occasional shaking. The reaction products together with a 15 ml of water were transferred into a separatory funnel with

CH_2Cl_2 via rinsing the vial (3 × 5 ml) and the internal standard was added (0.2 ml, 1 mg ml^{-1} octadecane in dioxane). The aqueous phase was adjusted to pH 3–4 by the addition of aqueous 0.4 M $NaHCO_3$ and the mixture was vigorously mixed. The aqueous phase was extracted twice with CH_2Cl_2. The combined CH_2Cl_2 fractions were dried over anhydrous Na_2SO_4, and then evaporated to dryness in a rotary evaporator at 40°C. The residue was completely redissolved in 1 ml of CH_2Cl_2 and 20 µl was trimethylsilylated with 50 µl with *N*,*O*-bis-(trimethylsilyl)-trifluoroacetamide (BSTFA) and 10 µl of pyridine. The GC analysis of the thioacidolysis monomers was performed with a gas chromatography-mass spectrometry (GCMS)-QP2010 Ultra instrument (Shimadzu, Japan) via a capillary column (DB-5HT, 30 m × 0.25 mm I.D. 0.10 µm film thickness). Temperature program: 50°C (1.5 min) → 90°C (2.0 min) at 30°C min^{-1}, → 250°C (8°C min^{-1}), 15 min holding time. The injector and transfer line temperatures were 250°C and 300°C, respectively. He was the carrier gas (1 ml min^{-1}). For dimer analysis, 0.9 ml of the CH_2Cl_2 solution containing the thioacidolysis products was subjected to a Raney-nickel desulfuration according to Lapierre et al. (1991). The dimeric compounds were trimethylsilylated with BSTFA and pyridine and then analyzed by GCMS on a Saturn 4000 (Varian, Walnut Creek, CA, USA) equipment. A short capillary column DB-5HT (12 m) was applied. The temperature program: 50°C → 90°C (2 min) at 30°C min^{-1}, 90°C → 250°C (8°C min^{-1}), holding time 2 min. The GCMS transfer line and injector temperatures were 300°C and 250°C, respectively, and He served as carrier gas (2 ml min^{-1}). Identification of dimers was done according to the literature (Lapierre et al. 1991; Rencoret et al. 2008; del Río et al. 2009; Kishimoto et al. 2010; Yue et al. 2017).

Results and discussion

The total lignin content of OTP (25%) was estimated as the sum of the Klason lignin (21%) and the acid soluble lignin (4%) contents. This value is similar to literature data (Toledano et al. 2011; Fillat et al. 2018).

2D-NMR of OTP and MWL

The OTP_{total} was analyzed *in situ* by 2D-HSQC in the gel state according to Kim et al. (2008) and Rencoret et al. (2009a), and the spectrum was compared with that of the MWL-OTP. The aliphatic-oxygenated (δ_C/δ_H 50–90/2.5–6.0) and the aromatic/unsaturated (δ_C/δ_H 100–155/5.8–7.8) regions of the HSQC spectra and that of MWL are presented in Figure 1. The HSQC spectrum of OTP_{total} (Figure 1a,b) reveal signals from carbohydrates and lignin. The former are dominated by hemicelluloses as cellulose signals cannot be detected in the gel state due to its high crystallinity (Kim et al. 2008). The main carbohydrate signals correspond to xylans (β-D-xylopyranoside X_2, X_3, X_4, X_5), including *O*-acetylated xylans (2- and 3-*O*-acetyl-β-D-xylopyranoside, X'_2 and X'_3), and 4-*O*-methyl-α-D-glucuronic acid (U_4). The signals in the MWL spectrum belong almost exclusively to lignin (Figure 1c,d). Although some modifications in lignin structure and its S/G ratio have been reported as a result of the isolation procedure (Balakshin et al. 2008; Capanema et al. 2015), comparison of the isolated MWL and the OTP_{total} spectra indicates that the former can be considered as representative of the native lignin in the OTP residue. The lignin correlation signals assigned in the HSQC spectra are listed in Table 1, and the lignin substructures identified are depicted in Figure 2.

The aliphatic-oxygenated region of the spectra gives information about the different inter-unit linkages of lignin. Here, the most intense correlation signals correspond to β-*O*-4′ alkyl aryl ethers (structure **A**) and methoxy groups of the benzene ring in G and S type lignin units. β-*O*-4′ linkages were found involving both G- and S- lignin units as two different C_β/H_β correlation signals are seen, depending on whether the 4′-*O*- is forming part of a guaiacyl ($A_{\beta(G)}$) or a syringyl ($A_{\beta(S)}$) lignin unit. Signals from carbon-carbon linkages, such as β-5′ phenylcoumarans (structure **B**) and β-β′ resinols (structure **C**), were also readily observed in the HSQC spectra of the OTP_{total} and the MWL. Interestingly, two clearly differentiated signals for the C_α/H_α correlations of β-5′ phenylcoumarans, at δ_C/δ_H 86.8/5.44 ($B_{\alpha(G)}$) and at δ_C/δ_H 87.7/5.59 ($B_{\alpha(S)}$), are detected only in the MWL spectrum. Although double phenylcoumaran C_α/H_α signals that could belong to phenolic and non-phenolic β-5′ structures can be observed in softwood lignin, in the OTP lignins they largely correspond to phenylcoumaran substructures involving G- or S-lignin units, as already shown for other hardwood lignins (Rencoret et al. 2018). Several signals are better resolved in the HSQC spectrum of MWL, such as 5-5′ dibenzodioxocins (structure **D**), and β-1′ spirodienones (structure **F**). The presence of dibenzodioxocin units is remarkable, which are important branching points in softwoods lignins (Karhunen et al. 1995), and which are seldom observed in hardwood lignins (Ämmälahti et al. 1998; Kukkola et al. 2004; Rencoret et al. 2009b). Dibenzodioxocin structures involve condensed 5-5 biphenyl C-C bonds, which are especially resistant to most chemical pretreatments, thus the reactivity of OTP lignin is probably lower than in other hardwoods.

In the aromatic/unsaturated region of the spectra, the typical correlation signals of S-, G-, and H-lignin units are seen, together with other signals from lignin end-groups, including cinnamyl alcohols (**I**) and cinnamaldehydes (**J**), and spirodienone substructures (**F**). According to the NMR data, OTP lignin is mainly composed of G- and S-lignin units in almost equal amounts (S/G ratio of 0.9–1.0), and with minor amounts of H-units (only 1–2% of the total lignin units).

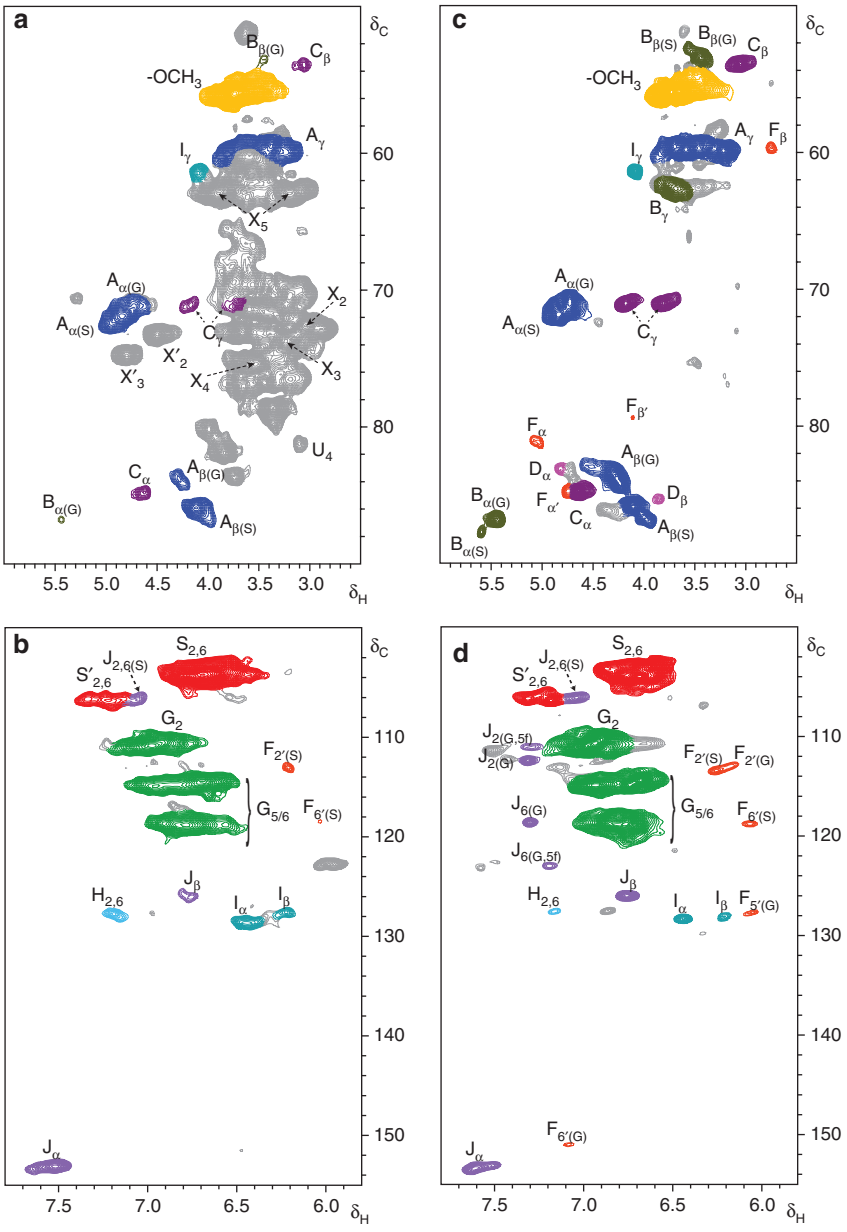

Figure 1: Side-chain (δ_C/δ_H 50–90/2.5–6.0, top) and aromatic/unsaturated (δ_C/δ_H 100–155/5.8–7.8, bottom) regions of the 2D HSQC NMR spectra of OTP_{total} (a and b) and OTP-MWL (c and d). The assignments of the lignin signals are listed in Table 1 and the lignin structures identified are depicted in Figure 2 .

The essential data estimated from the HSQC spectra of OTP_{total} and MWL are presented in Table 2, which include the quantification of inter-unit linkages and cinnamyl end-groups (as per 100 aromatic units, and as percentages of total linkages), the relative abundances of the H-, G-, and S-lignin units, and the S/G ratios. In general terms, the HSQC data indicate again that the MWL represents well the total lignin in the cell wall. It is also obvious that the MWL spectra have a higher resolution, an enhanced signal-to-noise ratio (i.e. minor lignin signals are detectable), and show correlation signals that appear overlapped with those from carbohydrates in the spectrum of OTP_{total}. In OTP lignin, the β-*O*-4′ alkyl-aryl ether linkages (**A**) are predominant accounting for 75% of the total detected inter-unit linkages, followed by β-5′ phenylcoumarans (12%), and β-β′ resinols (8%), together with lower proportions of β-1′ spirodienones (3%), and 5-5′ dibenzodioxocins (2%). Cinnamyl end-groups, including cinnamyl alcohols and cinnamaldehydes, accounted for 2 and 3% with respect to the total side-chains, respectively. The relatively high abundance of condensed (C-C) linkages, phenylcoumarans, dibenzodioxocins and G-lignin units (51%) are indicative that OTP lignin

Table 1: Assignments of the lignin $^{13}C/^{1}H$ correlation peaks in the 2D HSQC NMR spectra of olive tree (*Olea europaea*) pruning residues.

Label	δ_C/δ_H	Assignment
$B_{\beta(S)}$	52.4/3.56	C_β/H_β in phenylcoumarans (**B**) linked to S-units
$B_{\beta(G)}$	53.0/3.44	C_β/H_β in phenylcoumarans (**B**) linked to G-units
C_β	53.4/3.05	C_β/H_β in β-β′ resinols (**C**)
$-OCH_3$	55.5/3.73	C/H in methoxyls
A_γ	59.5/3.39 and 3.70	C_γ/H_γ in β-*O*-4′ alkyl-aryl ethers (**A**)
F_β	59.6/2.74	C_β/H_β in spirodienones (**F**)
I_γ	61.3/4.08	C_γ/H_γ in cinnamyl alcohol end-groups (**I**)
B_γ	62.6/3.69	C_γ/H_γ in phenylcoumarans (**B**)
$A_{\alpha(G)}$	70.9/4.72	C_α/H_α in β-*O*-4′ alkyl-aryl ethers (**A**) linked to G-units
C_γ	71.0/3.81 and 4.18	C_γ/H_γ in β-β′ resinols (**C**)
$A_{\alpha(S)}$	71.8/4.83	C_α/H_α in β-*O*-4′ alkyl-aryl ethers (**A**) linked to S-units
F'_β	79.3/4.10	C'_β/H'_β in spirodienones (**F**)
F_α	81.1/5.05	C_α/H_α in spirodienones (**F**)
D_α	83.1/4.81	C_α/H_α in 5-5′ dibenzodioxocins (**D**)
$A_{\beta(G)}$	83.8/4.26	C_β/H_β in β-*O*-4′ alkyl-aryl ethers (**A**) linked to G-units
F'_α	84.8/4.75	C'_α/H'_α in spirodienones (**F**)
C_α	84.8/4.65	C_α/H_α in β-β′ resinols (**C**)
D_β	85.3/3.84	C_β/H_β in 5-5′ dibenzodioxocins (**D**)
$A_{\beta(S)}$	86.3/4.03	C_β/H_β in β-*O*-4′ alkyl-aryl ethers (**A**) linked to S-units
$B_{\alpha(G)}$	86.8/5.44	C_α/H_α in phenylcoumarans (**B**) linked to G units
$B_{\alpha(S)}$	87.7/5.59	C_α/H_α in phenylcoumarans (**B**) linked to S-units
$S_{2,6}$	103.6/6.68	C_2/H_2 and C_6/H_6 in etherified syringyl units (**S**)
$J_{2,6(S)}$	106.2/7.04	C_2/H_2 and C_6/H_6 in sinapaldehyde end-groups (**J**)
$S'_{2,6}$	106.3/7.31 and 7.18	C_2/H_2 and C_6/H_6 in C_α-oxidized syringyl units (**S′**)
G_2	110.9/6.96	C_2/H_2 in guaiacyl units (**G**)
$J_{2(G,5f)}$	111.2/7.29	C_2/H_2 in coniferaldehyde end-groups C5-free (**J**)
$J_{2(G)}$	112.4/7.31	C_2/H_2 in coniferaldehyde end-groups C5-linked (**J**)
$F'_{2\,(G)}$	113.0/6.17	C'_2/H'_2 in guaiacyl spirodienones (**F**)
$F'_{2\,(S)}$	113.4/6.25	C'_2/H'_2 in syringyl spirodienones (**F**)
G_5/G_6	115.0/6.82	C_5/H_5 in guaiacyl units and C_6-H_6 in C5-linked guaiacyl units (**G**)
G_6	118.8/6.79	C_6/H_6 in guaiacyl units (**G**)
$J_{6(G)}$	118.7/7.30	C_6/H_6 in coniferaldehyde end-groups C5-linked (**J**)
$F'_{6(S)}$	118.8/6.07	C'_6/H'_6 in syringyl spirodienones (**F**)
$J_{6(G,5f)}$	123.0/7.19	C_6/H_6 in coniferaldehyde end-groups C5-free or β-*O*-4′ linked (**J**)
J_β	126.0/6.76	C_β/H_β in cinnamaldehyde end-groups (**J**)
$H_{2,6}$	127.6/7.17	C_2/H_2 and C_6/H_6 in *p*-hydroxyphenyl units (**H**)
$F'_{5(G)}$	127.7/6.05	C'_5/H'_5 in guaiacyl spirodienones (**F**)
I_β	128.2/6.21	C_β/H_β in cinnamyl alcohol end-groups (**I**)
I_α	128.4/6.44	C_α/H_α in cinnamyl alcohol end-groups (**I**)
$F'_{6(G)}$	151.1/7.09	C'_6/H'_6 in guaiacyl spirodienones (**F**)
J_α	153.5/7.61	C_α/H_α in cinnamaldehyde end-groups (**J**)

is probably less reactive than other hardwoods with higher S/G ratios and less C-C linkages, as, for example, in eucalyptus wood lignins (Rencoret et al. 2007, 2008; Prinsen et al. 2012). Lignocellulosic feedstocks with lower S/G lignin ratios are more difficult to delignify by alkaline pulping and therefore require higher amounts of alkali (Chang and Sarkanen 1973; Tsutsumi et al. 1995; del Río et al. 2005).

The 2D-NMR data demonstrate again the structural differences between the native lignin and the technical lignins of OTP by Santos et al. (2017). The lignins obtained from bioethanol production process (after steam explosion, followed by simultaneous saccharification and fermentation of the released sugars), contain less β-*O*-4′ alkyl-aryl ethers (49% of all detected linkages) and increased amounts of phenylcoumarans (15%) and, particularly, resinols (34%), because of the cleavage of β-*O*-4′ linkages during steam explosion (Santos et al. 2017). The lignins obtained after alkaline pulping of OTP suffered more severe degradation with a drastic decrease of all types of lignin linkages, particularly of β-*O*-4′ linkages, being resinols the only ones detected in alkaline lignins, which also have more phenolic content (Santos et al. 2017).

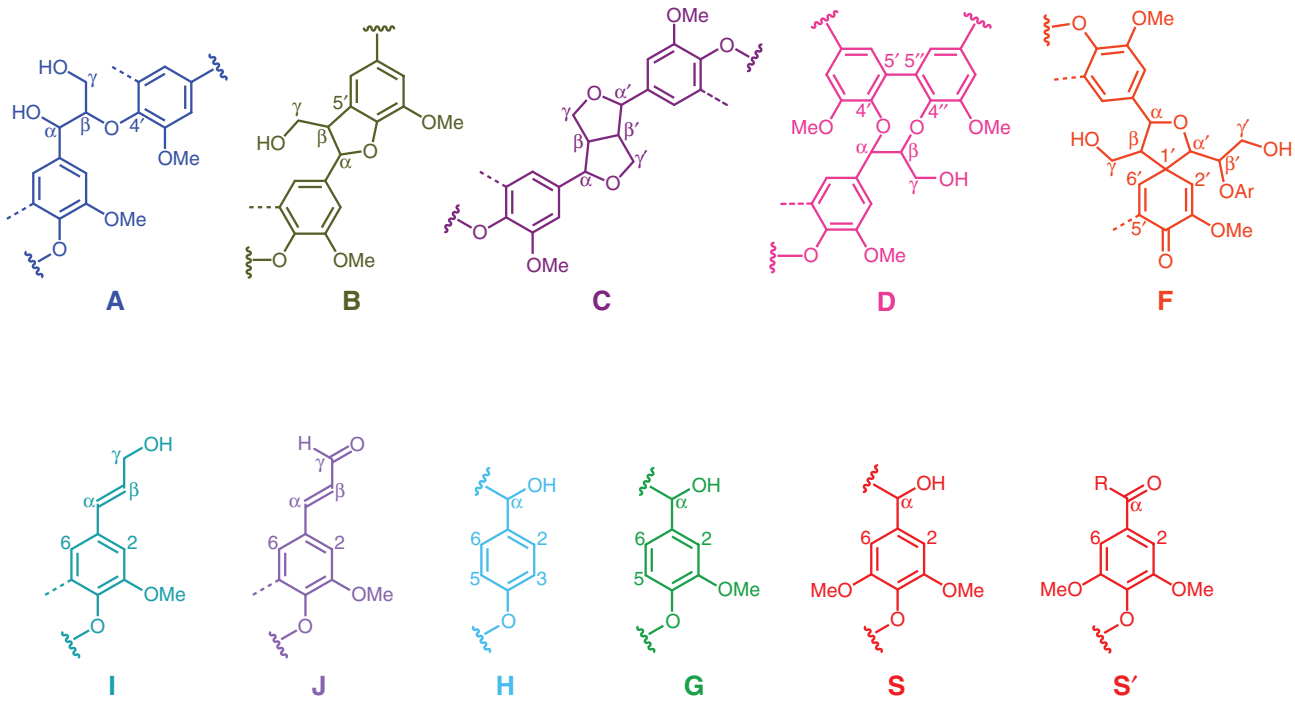

Figure 2: Main lignin structures and units identified in the 2D HSQC NMR spectra of OTP_{total} and OTP-MWL: β-*O*-4′ alkyl-aryl ethers (**A**); β-5′ phenylcoumarans (**B**); β-β′ resinols (**C**); 5-5′ dibenzodioxocins (**D**); β-1′ spirodienones (**F**); cinnamyl alcohol end-groups (**I**); cinnamaldehyde end-groups (**J**); *p*-hydroxyphenyl units (**H**); guaiacyl units (**G**); syringyl units (**S**); Cα-oxidized syringyl units (**S′**).

The technical lignins recovered after bioethanol or alkaline pulping were highly enriched in syringyl units (S/G ratios around 4.0–5.7) compared with the native lignin (S/G around 1), most probably due to the enrichment of resinol substructures.

Table 2: Main structural characteristics, including the abundance of lignin inter-unit linkages expressed as linkages per 100 aromatic units (relative percentages of the total inter-unit linkages are also provided in parentheses), end-groups referred to the total side-chains, aromatic units and S/G ratios, determined by integration of $^{13}C/^{1}H$ correlation peaks in the HSQC spectra of the OTP_{total} and the OPT-MWL.

Units, linkages	OTP_{total}	MWL
Inter-unit linkages		
β-*O*-4′ aryl ethers (**A**)	53 (79)	52 (75)
β-5′ Phenylcoumarans (**B**)	8 (12)	9 (12)
β-β′ Resinols (**C**)	6 (9)	6 (8)
5-5′ Dibenzodioxocins (**D**)	– (–)	1 (2)
β-1′ Spirodienones (**F**)	– (–)	1 (3)
Lignin end-groups		
Cinnamyl alcohol end-groups (**I**)	4	2
Cinnamaldehyde end-groups (**J**)	2	3
Aromatic units		
H (%)	2	1
G (%)	48	51
S (%)	50	48
S/G ratio	1.0	0.9

Analysis of lignin monomers and condensed linkages

2D-HSQC provided semiquantitative information regarding the lignin composition and the main inter-unit linkages. The data with this regard obtained by thioacidolysis are quantitative, where the yields of monomeric products are indicative for the selective cleavage of β-*O*-4′ linkages. The analysis of dimeric products gives information on the 'condensed' (C-C) and diaryl ether linkages including 5-5′, 4-*O*-5′, β-1′, β-5′, and β-β′ linkages. The chromatogram in Figure 3 shows the monomeric thioacidolysis degradation

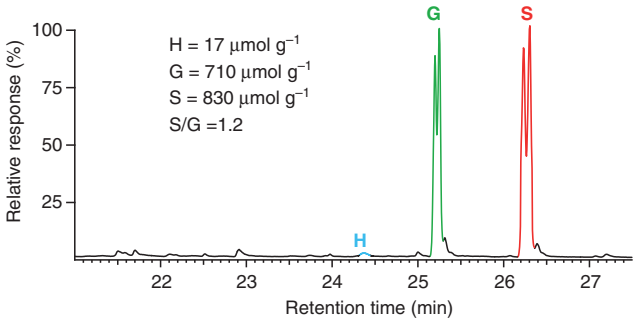

Figure 3: Total ion chromatogram of the monomeric thioacidolysis degradation products (as TMS ethers) released from OTP-MWL.

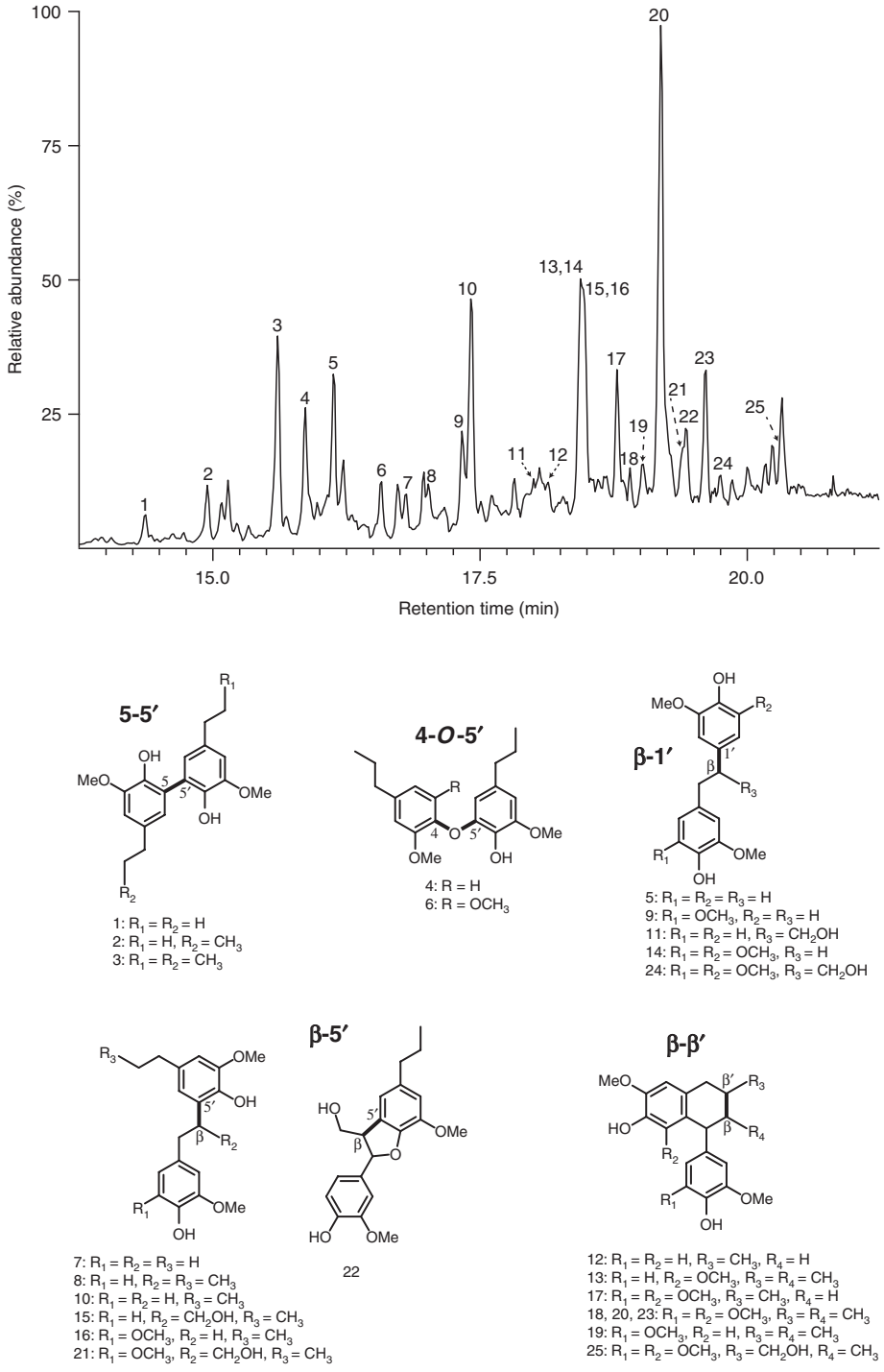

Figure 4: Total ion chromatogram of the dimeric products (as TMS ethers) obtained by thioacidolysis degradation followed by Raney-nickel desulphuration of OTP-MWL.
The mass spectral data are detailed in Table 3.

products as TMS ether derivatives. Thioacidolysis released similar amounts of G and S type units (710 and 830 μmoles g^{-1} lignin, respectively), with small amounts of H monomers (17 μmoles g^{-1} lignin), as already observed by 2D-NMR. As expected, the S/G ratio of 1.2 obtained upon thioacidolysis was slightly higher than that estimated by 2D-NMR, as thioacidolysis only releases lignin monomers involved in β-*O*-4′ bonds, which are more abundant among

Table 3: Identification, mass spectral fragments (base peaks are underlined) and relative molar abundances of the dimeric products (as TMS ethers) released after thioacidolysis followed by Raney-nickel desulfuration of OTP-MWL.

Peak	Dimeric compound	M_w	Main fragments	Rel. abund. (%)
1	5-5′ (G-G)	446	446, 431, 417, 416, 73	1.3
2	5-5′ (G-G)	460	460, 445, 431, 430, 73	2.5
3	5-5′ (G-G)	474	474, 459, 445, 444, 73	9.5
4	4-*O*-5′ (G-G)	402	402, 387, 373, 372, 73	5.3
5	β-1′ (G-G)	418	418, 209, 179, 73	5.2
6	4-*O*-5′ (G-S)	432	432, 417, 403, 402, 73	2.5
7	β-5′ (G-G)	446	446, 222, 209, 207, 179, 73	1.4
8	β-5′ (G-G)	474	474, 265, 234, 209, 73	1.2
9	β-1′ (G-S)	448	448, 239, 209, 179, 73	3.7
10	β-5′ (G-G)	460	460, 251, 209, 207, 179, 73	10.0
11	β-1′ (G-G, -OH)	520	520, 311, 223, 209, 73	0.4
12	β-β′ (G-G)	472	472, 385, 276, 73	0.7
13	β-β′ (G-S)	502	502, 306, 239, 209, 73	3.3
14	β-1′ (S-S)	478	478, 463, 239, 209, 73	6.8
15	β-5′ (G-G, -OH)	562	562, 472, 263, 209, 191, 73	1.8
16	β-5′ (G-S)	490	490, 239, 209, 207, 191, 73	7.1
17	β-β′ (S-S)	518	518, 503, 488, 292, 262, 73	3.9
18	β-β′ (S-S)	532	532, 517, 445, 306, 291, 275, 73	1.1
19	β-β′ (G-S)	502	502, 487, 472, 415, 276, 73	1.6
20	β-β′ (S-S)	532	532, 517, 445, 306, 291, 275, 73	20.5
21	β-5′ (G-S,-OH)	592	592, 502, 472, 239, 209, 191, 73	1.8
22	β-5′ (G-G), coumarans	488	488, 458, 398, 368, 209, 73	2.0
23	β-β′ (S-S)	532	532, 517, 445, 306, 291, 275, 73	4.9
24	β-1′ (S-S,-OH)	580	580, 530, 341, 239, 209, 73	0.8
25	β-β′ (S-S)	620	620, 605, 499, 354, 266, 239, 73	0.7

the syringyl units. Therefore, it should be indicated that the thioacidolysis data underestimates the amount of the condensed units.

The chromatogram of the thioacidolysis dimeric products (as TMS ethers) is shown in Figure 4, together with their structures, and their mass spectral data, and their relative abundances are summarized in Table 3. The main dimeric compounds released are of the type 5-5′ (peaks 1–3), 4-*O*-5′ (peaks 4 and 6), β-1′ (peaks 5, 9, 11, 14 and 24), β-5′ (peaks 7, 8, 10, 15, 16, 21 and 22), and β-β′ (peaks 12, 13, 17–19 and 25). The 5-5′ dimers arise in part from dibenzodioxocin structures after the breakdown of their α-*O*-4′ and β-*O*-4′′ ethers, and also from others 5-5′ etherified and non-etherified units (Capanema et al. 2004). The β-1′ dimers are produced from spirodienones after the cleavage of the α-*O*-α′ ether bond whereas the β-β′ tetralin dimers arise from the cleavage of α-*O*-γ ether bonds in resinols and subsequent recyclization through the formation of an additional bond between Cα and C_6 (Lapierre et al. 1995). Two types of β-5′ dimers were detected: (1) those simply derived from an unopened phenylcoumaran, such as dimer 22 that was recently established as authentic β-5′ dimer by synthesized standards (Yue et al. 2017), and (2) those β-5′ dimers arising from the breakdown of α-*O*-4′ ether in phenylcoumaran substructures (dimers 7, 8, 10, 15, 16 and 21).

The relative proportions of the different dimers released upon thioacidolysis-desulfuration are listed in Table 4. The quantity of the most prominent dimers (based on all dimers) are β-β′ tetralin (≈37%) and β-5′ compounds (≈25%), followed by β-1′ (≈17%), 5-5′ (≈13.3%) and 4-*O*-5′ (≈7.8%) structures. 2D-NMR analysis, however, showed a higher abundance of β-5′ than β-β′ structures in OTP lignin. One possible explanation is that β-5′ linkages occur among G units (65% of all β-5′ dimers involve two G-units), that

Table 4: Relative molar percentages of the different dimer types (see Table 3 and Figure 4) released by thioacidolysis and Raney-nickel desulfuration of OTP-MWL.

	Basic units (mol %)		
Linkage	GG	SG	SS
5-5′	13.3		
4-O-5′	5.3	2.5	
β-1′	5.6	3.7	7.6
β-5′	16.4	8.9	
β-β′	0.7	4.9	31.1

can also be connected to other lignin units, which are not degraded by thioacidolysis resulting in underrepresented β-5′ substructures among thioacidolysis degradation products. On the contrary, the vast majority of the β-β′ linkages in OTP lignin are of the S-S type (85% of all β-β′ linkages) (Table 4). This observation is also true for lignins in other plants (Rencoret et al. 2008; del Río et al. 2009). Such S-S dimers can only be integrated into the lignin macromolecule via their 4-OH groups, which leads to formation of β-*O*-4′ alkyl-aryl ethers, which are cleaved by thioacidolysis. β-β′ resinols are mainly syringaresinol and this could explain the high S/G ratios of OTP technical lignins obtained by steam explosion and alkaline pulping (Santos et al. 2017), because these pretreatments mostly cleave β-*O*-4′ linkages and produce a lignin highly enriched in β-β′ resinols.

Conclusions

The characterization of the MWL isolated from OTP has revealed that it belongs to the SG lignin type with a S/G ratio of ≈1, whereas H units were found only in low amounts. The main lignin inter-units linkages included β-*O*-4′ alkyl-aryl ethers, followed by β-5′ phenylcoumarans, and β-β′ resinols, and with lower amounts of β-1′ spirodienones, 5-5′ dibenzodioxocins, and 4-*O*-5′ aryl-aryl ethers. In general terms, the relative high lignin content (≈25%), together with ca. 50% G units, which are responsible for the important content of condensed substructure, would make OTP, a priori, more recalcitrant to pretreatments. A better knowledge of the OTP lignin structure will help maximizing the utilization of this agricultural residue and develop appropriate industrial processes for its valorization.

Acknowledgements: We are grateful to Dr. Manuel Angulo (CITIUS, University of Seville) for technical assistance with the NMR experiments.

Author contributions: All the authors have accepted responsibility for the entire content of this submitted manuscript and approved submission.

Research funding: This study has been funded by the Spanish projects CTQ2014-60764-JIN and AGL2017-83036-R (financed by Agencia Estatal de Investigación, AEI, and Fondo Europeo de Desarrollo Regional, FEDER), and the CSIC project 2014-40E-097.

Employment or leadership: None declared.

Honorarium: None declared.

References

Ämmälahti, E., Brunow, G., Bardet, M., Robert, D., Kilpeläinen, I. (1998) Identification of side-chain structures in a poplar lignin using three-dimensional HMQC-HOHAHA NMR spectroscopy. J. Agric. Food Chem. 46:5113–5117.

Balakshin, M.Y., Capanema, E.A., Chang, H.-M. (2008) Recent advances in the isolation and analysis of lignins and lignin–carbohydrate complexes. In: Characterization of lignocellulosic materials. Ed. Hu, T. Blackwell, Oxford, UK. pp. 148–170.

Björkman, A. (1956) Studies on finely divided wood. Part I. Extraction of lignin with neutral solvents. Sven. Papperstidn. 59:477–485.

Boerjan, W., Ralph, J., Baucher, M. (2003) Lignin biosynthesis. Ann. Rev. Plant Biol. 54:519–546.

Capanema, E.A., Balakshin, M.Y., Kadla, J.F. (2004) A comprehensive approach for quantitative lignin characterization by NMR spectroscopy. J. Agric. Food Chem. 52:1850–1860.

Capanema, E.A., Balakshin, M.Y., Katahira, R., Chang, H.-M., Jameel, H. (2015) How well do MWL and CEL preparations represent the whole hardwood lignin? J. Wood Chem. Technol. 35:17–26.

Cara, C., Ruiz, E., Ballesteros, M., Manzanares, P., Negro, M.J., Castro, E. (2008) Production of fuel ethanol from steam-explosion pretreated olive tree pruning. Fuel 87:692–700.

Chang, H.M., Sarkanen, K.V. (1973) Species variation in lignin: effect of species on the rate of Kraft delignification. Tappi 56:132–136.

del Río, J.C., Gutiérrez, A., Hernando, M., Landín, P., Romero, J., Martínez, Á.T. (2005) Determining the influence of eucalypt lignin composition in paper pulp yield using Py-GC/MS. J. Anal. Appl. Pyrol. 74:110–115.

del Río, J.C., Rencoret, J., Marques, G., Li, J., Gellerstedt, G., Jiménez-Barbero, J., Martínez, Á.T., Gutiérrez, A. (2009) Structural characterization of the lignin from jute (*Corchorus capsularis*) fibers. J. Agric. Food Chem. 57:10271–10281.

del Río, J.C., Prinsen, P., Rencoret, J., Nieto, L., Jiménez-Barbero, J., Ralph, J., Martínez, Á.T., Gutiérrez, A. (2012) Structural characterization of the lignin in the cortex and pith of elephant grass (*Pennisetum purpureum*) stems. J. Agric. Food Chem. 60:3619–3634.

Díaz, M.J., Huijgen, W.J.J., van der Laan, R.R., Reith, J.H., Cara, C., Castro, E. (2011) Organosolv pretreatment of olive tree biomass for fermentable sugars. Holzforschung 65:177–183.

FAOSTAT (2016) http://www.fao.org/faostat/en/#data/QC. (Accessed 26/2/2018).

Fillat, U., Wicklein, B., Martín-Sampedro, R., Ibarra, D., Ruiz-Hitzky, E., Valencia, C., Sarrión, A., Castro, E., Eugenia, M.E. (2018) Assessing cellulose nanofiber production from olive tree pruning residue. Carbohydr. Polym. 179:252–261.

Fujimoto, A., Matsumoto, Y., Chang, H.M., Meshitsuka, G. (2005) Quantitative evaluation of milling effects on lignin structure during the isolation process of milled wood lignin. J. Wood Sci. 51:89–91.

Himmel, M.E. Biomass Recalcitrance. Deconstructing the Plant Cell Wall for Bioenergy. Blackwell, Oxford, 2008.

Karhunen, P., Rummakko, P., Sipilä, J., Brunow, G., Kilpeläinen, I. (1995) Dibenzodioxocins – A novel type of linkage in softwood lignins. Tetrahedron Lett. 36:169–170.

Kim, H., Ralph, J., Akiyama, T. (2008) Solution-state 2D NMR of ball-milled plant cell wall gels in DMSO-d_6. Bioenerg. Res. 1:56–66.

Kishimoto, T., Chiba, W., Saito, K., Fukushima, K., Uraki, Y., Ubukata, M. (2010) Influence of syringyl to guaiacyl ratio on the structure of natural and synthetic lignins. J. Agric. Food Chem. 58:895–901.

Kukkola, E., Koutaniemi, S., Pöllänen, E., Gustafsson, M., Karhunen, P., Lundell, T.K., Saranpää, P., Kilpeläinen, I, Teeri, T.H., Fagerstedt, K.V. (2004) The dibenzodioxocin lignin substructure is abundant in the inner part of the secondary wall in Norway spruce and silver birch xylem. Planta 218:497–500.

Lapierre, C., Pollet, B., Monties, B., Rolando, C. (1991) Thioacidolysis of spruce lignin: gas chromatography-mass spectroscopy analysis of the main dimers recovered after Raney nickel desulfurization. Holzforschung 45:61–68.

Lapierre, C., Pollet, B., Rolando, C. (1995) New insights into the molecular architecture of hardwood lignins by chemical degradative methods. Res. Chem. Intermed. 21:397–412.

Lourenço, A., Rencoret, J., Chemetova, C., Gominho, J., Gutiérrez, A., Pereira, H., del Río, J.C. (2015) Isolation and structural characterization of lignin from cardoon (*Cynara cardunculus* L.) stalks. Bioenergy Res. 8:1946–1955.

Prinsen, P., Gutiérrez, A., Rencoret, J., Nieto, L., Jiménez-Barbero, J., Burnet, A., Petit-Conil, M., Colodette, J.L., Martínez, A.T., del Río, J.C. (2012) Morphological characteristics and composition of lipophilic extractives and lignin in Brazilian woods from different eucalypt hybrids. Ind. Crops Prod. 36:572–583.

Ragauskas, A.J., Williams, C.K., Davison, B.H., Britovsek, G., Cairney, J., Eckert, C.A., Frederick, W.J., Hallett, J.P., Leak, D.J., Liotta, C.L., Mielenz, J.R., Murphy, R., Templer, R., Tschaplinski. T. (2006) The path forward for biofuels and biomaterials. Science 311:484–489.

Ralph, J., Lundquist, K., Brunow, G., Lu, F., Kim, H., Schatz, P.F., Marita, J.M., Hatfield, R.D., Ralph, S.A., Christensen, J.H., Boerjan, W. (2004) Lignins: natural polymers from oxidative coupling of 4-hydroxyphenylpropanoids. Phytochem. Rev. 3:29–60.

Ralph, S.A., Landucci, L.L., Ralph, J. (2009) NMR database of lignin and cell wall model compounds. Available at https://www.glbrc.org/databases_and_software/nmrdatabase. (Accessed: 2 November 2011).

Rencoret, J., Gutiérrez, A., del Río, J.C. (2007) Lipid and lignin composition of woods from different eucalypt species. Holzforschung 61:165–174.

Rencoret, J., Marques, G., Gutiérrez, A., Ibarra, D., Li, J., Gellerstedt, G., Santos, J.I., Jiménez-Barbero, J., Martínez, Á.T., del Río, J.C. (2008) Structural characterization of milled wood lignins from different eucalypt species. Holzforschung 62:514–526.

Rencoret, J., Marques, G., Gutiérrez, A., Nieto, L., Santos, J.I., Jiménez-Barbero, J., Martínez, Á.T., del Río, J.C. (2009a) HSQC-NMR analysis of lignin in woody (*Eucalyptus globulus* and *Picea abies*) and non-woody (*Agave sisalana*) ball-milled plant materials at the gel state. Holzforschung 63:691–698.

Rencoret, J., Marques, G., Gutiérrez, A., Nieto, L., Jiménez-Barbero, J., Martínez, A.T., del Río, J.C. (2009b) Isolation and structural characterization of the milled wood lignin from *Paulownia fortunei* wood. Ind. Crops Prod. 30:137–143.

Rencoret, J., Ralph, J., Marques, G., Gutiérrez, A., Martínez, Á.T., del Río, J.C. (2013) Structural characterization of lignin isolated from coconut (*Cocos nucifera*) coir fibers. J. Agric. Food Chem. 61:2434–2445.

Rencoret, J., Kim, H., Evaristo, A.B., Gutiérrez, A., Ralph, J., del Río, J.C. (2018) Variability in lignin composition and structure in cell walls of different parts of macaúba (*Acrocomia aculeata*) palm fruit. J. Agric. Food Chem. 66:138–153.

Rolando, C., Monties, B., Lapierre, C. (1992) Thioacidolysis. In: Methods in Lignin Chemistry. Eds. Dence, C.W., Lin, S.Y. Springer-Verlag, Berlin-Heidelberg. pp. 334–349.

Romero, I., Ruiz, E., Castro, E., Moya, M. (2010) Acid hydrolysis of olive tree biomass. Chem. Eng. Res. Des. 88:633–640.

Sánchez, S., Moya, A.J., Moya, M., Romero, I., Torrero, R., Bravo, V., San Miguel, M.P. (2002) Aprovechamiento del residuo de poda del olivar. Ing. Quím. 34:194–202.

Santos, J.I., Fillat, Ú., Martín-Sampedro, R., Eugenio, M.E., Negro, M.J., Ballesteros, I., Rodríguez, A., Ibarra, D. (2017) Evaluation of lignins from side-streams generated in an olive tree pruning-based biorefinery: bioethanol production and alkaline pulping. Int. J. Biol. Macromol. 105:238–251.

Sequeiros, A., Labidi, J. (2017) Characterization and determination of the S/G ratio via Py-GC/MS of agricultural and industrial residues. Ind. Crops Prod. 97:469–476.

Tappi. Tappi Test Methods 2004–2005. Tappi Press, Norcoss, GA 30092 USA, 2004.

Toledano, A., Serrano, L., Labidi, J. (2011) Enhancement of lignin production from olive tree pruning integrated in a green biorefinery. Ind. Eng. Chem. Res. 50:6573–6579.

Toledano, A., Erdocia, X., Serrano, L., Labidi, J. (2013a) Influence of extraction treatment on olive tree (*Olea europaea*) pruning lignin structure. Environ. Prog. Sustain. Energy 32:1187–1194.

Toledano, A., Serrano, L., Labidi, J. (2013b) Extraction and revalorization of olive tree (*Olea europea*) pruning lignin. J. Taiwan Inst. Chem. Eng. 44:552–559.

Tsutsumi, Y., Kondo, R., Sakai, K., Imamura, H. (1995) The difference of reactivity between syringyl lignin and guaiacyl lignin in alkaline systems. Holzforschung 49:423–428.

Yue, F., Lu, F., Regner, M., Sun, R., Ralph, J. (2017) Lignin-derived thioacidolysis dimers: reevaluation, new products, authentication, and quantification. ChemSusChem 10:830–835.

Zobel, B.J., van Buijtenen, J.P. Wood Variation. Its Causes and Control. Springer-Verlag, Heidelberg, Germany, 1989.